

## Band structure of carbonated amorphous silicon studied by optical, photoelectron, and x-ray spectroscopy

I. Solomon and M. P. Schmidt\*

*Laboratoire de Physique de la Matière Condensée, Ecole Polytechnique, 91128 Palaiseau CEDEX, France*

C. Sénémaud and M. Driss Khodja

*Laboratoire de Chimie Physique, Université Pierre et Marie Curie (Paris VI), 11 rue Pierre et Marie Curie, 75231 Paris CEDEX 05, France*

(Received 26 July 1988)

Hydrogenated silicon-carbon films prepared by glow discharge from silane-methane mixtures at low power density are used as a model system for the analysis of optical properties and band structure of amorphous tetrahedral semiconductors. Between 0 and 20 at. % of carbon in the solid, the optical gap and the static refractive index can be varied over a wide range without changing the chemical structure of the solid and its good semiconducting properties. The optical constants are well described by a simple two-band model of optical transitions, and the information on the band structure in the solid is condensed into one parameter, the average gap  $E_M$ , which corresponds to the energy difference between the centers of gravity of the valence and conduction bands. This value is very close to the energy spacing of the maxima in the distributions of the conduction and valence band deduced from soft-x-ray spectra, and exhibits a similar increase with carbon content. Beyond a carbon concentration of about 20 at. %, we observe a change in the nature of the material. The average gap  $E_M$  increases much more rapidly than the optical gap; x-ray photoelectron spectroscopy indicates an incorporation of carbon in the form of Si-C-Si units in a tetrahedral network, whereas for concentrations smaller than 20 at. % the carbon is mainly incorporated as methyl groups  $\text{CH}_3$ .

### I. INTRODUCTION

The optical properties and the band structure of amorphous hydrogenated silicon have been studied extensively during the past ten years. Several correlations between optical parameters that seem to apply to a great variety of *a*-Si:H films have been found: the refractive index at infinite wavelength shows a linear decrease with the optical gap,<sup>1</sup> and the optical gap increases with the hydrogen content of the film.<sup>2,3</sup> A detailed analysis of optical matrix elements suggests that the optical properties of *a*-Si:H can be represented to first order by a two-band model with a resonant energy of 3.4–3.6 eV and a damping factor of 4 eV.<sup>4</sup> However, these results are difficult to interpret in terms of general principles of tetrahedral semiconductors, since the range of optical properties that can be obtained with *a*-Si:H prepared under different conditions is rather limited. An ideal model system should be able to account for a wide range of optical properties without discontinuous changes of chemical and band structure, while disorder and defect density remain at a constant level.

Indeed, the optical band gap of amorphous silicon can be modified if other elements like carbon, germanium, or tin are added during preparation. Unfortunately, chemical bonding and band structure of these amorphous IV-IV alloys depend not only on film composition but also on preparation conditions. For systematic studies of composition-dependent effects, this poses a problem since

the observed changes in the film properties cannot unambiguously be attributed to composition changes. In the case of glow-discharge deposition, the admixture of germane or other gases with silane generally changes the plasma chemistry drastically. For instance, important variations of growth rate as a function of gas composition at constant rf power have been reported in the literature for mixtures of silane with methane,<sup>5</sup> ethylene,<sup>6</sup> tetramethylsilane,<sup>7</sup> and germane.<sup>8</sup> In these cases, the variation of one deposition parameter may have a stronger influence on film properties than the composition-dependent effect to be studied. The only exception known so far is amorphous silicon-carbon alloys<sup>9</sup> which can be prepared, under certain conditions, as well-defined standard materials over a fairly wide range of compositions. Two different deposition regimes have been identified for glow-discharge decomposition of silane-methane mixtures, depending on the power density:<sup>10,11</sup> at low power density, there is practically no primary decomposition of methane by electron impact and methane decomposition occurs mainly via reactive species formed by silane decomposition. The deposition rates from pure methane are negligible under these conditions. The maximum carbon content in the solid is about 40 at. %, obtained by extrapolation to the limit of 100 at. % methane concentration in the gas phase.

It has been shown that the low-power-density regime provides a smooth incorporation of carbon into the silicon network, mainly in the form of methyl groups  $\text{CH}_3$ ,

giving an alloy with good semiconducting properties as verified, for example, by a low density of states in the mobility gap.<sup>12</sup> The material obtained in this fashion has well-defined optical properties which depend almost exclusively on gas concentration and are highly insensitive to the preparation conditions. These conditions are very close to those used for device-quality *a*-Si:H. In contrast, at high power density, both methane and silane are decomposed by electron impact, and film properties depend strongly on preparation conditions like substrate temperature, total pressure, dilution, and flow rate.<sup>5</sup> Amorphous silicon-carbon films produced under low-power-density conditions show a wide range of optical gaps, from 1.7 to 2.8 eV.<sup>11</sup> At the same time, structural disorder increases only modestly and the electrical properties remain comparable to those of *a*-Si:H. They seem, therefore, to be a good model system for fundamental studies of band structure and its dependence on composition. In particular, the different models of optical band-to-band transitions responsible for the dispersion of the refractive index can be tested.

In the present paper, we investigate the effect of low-power carbon incorporation into amorphous silicon by means of x-ray photoemission spectroscopy (XPS) and soft-x-ray spectroscopy (SXS). From optical spectra, we deduce characteristic band-gap energies which indicate a widening of the band gap upon carbon incorporation. This effect is also studied by soft-x-ray emission and absorption spectroscopy which probe the valence- and conduction-band states around silicon atoms having a *p* symmetry. Core-level Si 2*p* and C 1*s* distributions which contain information on chemical bonding have been analyzed by photoelectron spectroscopy. Some preliminary results on this work have been presented in a previous communication.<sup>13</sup> After a brief description of the experimental techniques (Sec. II), we show in Sec. III that for a wide range of optical band-gap values, the experimentally observed dispersion of the refractive index can be represented by a simple one-oscillator model. This approach leads to the definition of an "average gap" similar to the Penn gap,<sup>14</sup> which turns out to be an important parameter that characterizes the band structure in *a*-Si:H alloys. We find that this average gap roughly corresponds to the energy difference between the maxima in the density of states of the valence and conduction bands as deduced from soft-x-ray spectra.

## II. EXPERIMENTAL

Amorphous carbonated silicon films were deposited by glow-discharge decomposition of methane-silane mixtures at low power densities using a capacitively coupled rf reactor previously described.<sup>2</sup> Methane concentrations in the gas phase ranged from 0 to 95 at. %. The power density was 0.1 W/cm<sup>2</sup>. In the limit of the low-power-density regime, the concentration of methane governs the optical properties of the deposited films. The other deposition parameters are of marginal importance; they have been specified in Table I for the sake of completeness.

The substrates used for this work are glass for optical transmission, aluminum for x-ray emission, beryllium foil

TABLE I. Deposition parameters. (sccm denotes cubic centimeters per minute at STP.)

Substrate temperature	250°C
Pressure	40 mTorr
Gas-flow rate	20 sccm
[CH <sub>4</sub> ]/([CH <sub>4</sub> ] + [SiH <sub>4</sub> ])	0–95 at. %
rf power density	0.1 W/cm <sup>2</sup>
rf frequency	13.56 MHz

for x-ray absorption, and molybdenum foil for photoelectron spectroscopy. The film thickness was usually 0.8 μm except for XPS where 0.1-μm-thick films were deposited. The carbon content of the films has been determined by means of Auger-electron spectroscopy and XPS; both methods were calibrated using films of different compositions for which independent chemical analysis using techniques other than surface spectroscopy had been performed in specialized laboratories. A comparison of these results is given elsewhere.<sup>11</sup>

Optical-absorption coefficients and refractive indices were computed from transmission spectra recorded on a commercial spectrophotometer in the 400–1100-nm range. Soft-x-ray spectra were recorded using bent-crystal spectrometers [second-order reflection on gypsum (020) crystal sheets] equipped with a photographic detector (emulsion Kodak SA3). Further experimental details have been described elsewhere.<sup>15</sup> The energy resolution  $dE/E$  was  $2 \times 10^{-4}$ , the instrumental broadening being of the order of 0.3 eV. For SXS studies natural oxides on the surface were not stripped prior to measurement. The effective sample thickness involved in emission spectra was about 0.3 μm in our experimental conditions. For absorption spectra, the total thickness of the sample is probed. Consequently, the contribution of surface contamination to the x-ray spectra is negligible. Photoelectron spectra were induced by monochromatic Al *Kα*<sub>1,2</sub> radiation with  $h\nu = 1486.6$  eV (spectral width 0.3 eV) which gives a total instrumental broadening of about 0.5 eV. No charge effect was observed for our samples. Binding energies were evaluated with reference to the Au 4*f*<sub>7/2</sub> level at 83.8 eV. Spectra were decomposed numerically by a fit based on the addition of Gaussian distributions. In these experiments, the effective sample thickness was only a few tens of angstroms. Samples for XPS spectra were sputter cleaned with 900-eV Ar<sup>+</sup> ions. In order to minimize argon implantation, the sputter cleaning was not complete: although most of the surface contamination was removed, some of the surface oxide subsisted. One of the *a*-Si<sub>1-x</sub>C<sub>x</sub> samples was protected by a thin overlayer of *a*-Si:H which was eliminated in the spectrometer by sputtering. During all measurements, the pressure in the XPS spectrometer was below 10<sup>-8</sup> Torr.

## III. RESULTS

### A. Determination of optical constants

Optical transmission spectra of homogeneous thin films contain all the information necessary to calculate the film

thickness  $d$ , the refractive index  $n$ , and the absorption coefficient  $\alpha$ . We have developed a computer program which calculates the thickness and refractive index at different wavelengths from the envelope of the interference fringes of the transmission spectrum corrected for absorption in the substrate. Our method is similar to that described in detail by Perrin<sup>16</sup> and by Swanepoel.<sup>17</sup> It makes it possible to compute the optical constants at any wavelength within the range of measurement. The accuracy of the optical constants so obtained is better than 1%. The values for the film thickness calculated from the optical transmission spectra are within experimental error equal to those obtained with commercially available stylus instruments.

For the determination of the optical gap, we avoid the use of the conventional Tauc plot which requires a rather ill-defined extrapolation subject to relatively large statistical errors. Instead, we evaluate the energy  $E_{04}$  at which the absorption coefficient equals  $10^4 \text{ cm}^{-1}$ . This energy is about 0.15 eV higher than the Tauc gap for carbonated amorphous silicon<sup>12</sup> and is insignificant for the discussion of our experimental results. In the transparent region ( $E < E_{04}$ ), the experimental variation of  $n$  with wavelength can be represented by a simple quadratic variation like

$$n(\lambda) = n_0(1 + \lambda_t^2/\lambda^2), \quad (1)$$

where the refractive index at infinite wavelength  $n_0$  and the characteristic energy  $\lambda_t$  are obtained from a fit.

### B. The dispersion of the refractive index: The "average gap model"

Even though the dispersion of the refractive index of our samples can be described by the simple equation above, it is difficult to attribute a physical meaning to it. We therefore consider another expression which can be related to physical parameters in a more straightforward way. The real part of the electronic dielectric constant in most covalent and ionic solids can be written as

$$\epsilon_1(\omega) = 1 + \frac{e^2}{\pi^2 m} \sum_{i,j} \int_{\text{BZ}} d\mathbf{k} \frac{f_{ij}^\alpha(\mathbf{k})}{\omega_{ij}^2(\mathbf{k}) - \omega^2}, \quad (2)$$

where  $e$  and  $m$  are, respectively, the electronic charge and mass. The sum extends over all bands  $i$  and  $j$  such that  $i \neq j$ , and the integral extends over the Brillouin zone (BZ). For each transition between two bands  $i$  and  $j$ , the oscillator strength for a polarization of direction  $\alpha$  is given by  $f_{ij}^\alpha(\mathbf{k})$ . In order to reduce Eq. (2) to macroscopic parameters that can be determined experimentally, isotropic two-band models, in spite of their simplicity, have been found to be a very good approximation in many nonmetallic crystals.<sup>14,18</sup> Isotropic models should be particularly well suited to amorphous solids due to the absence of long-range order. With Wemple and DiDomenico's extremely simplified model,<sup>18</sup> it can be shown that Eq. (2) can be reduced to a one-oscillator formula describing the dielectric response for subgap transitions:

$$\epsilon_1(E) = n^2(E) = 1 + (n_0^2 - 1) \frac{E_M^2}{E_M^2 - E^2}. \quad (3)$$

The quantity  $n(E)$  is the value of the refractive index at the photon energy  $E$ ,  $n_0$  is the refractive index extrapolated to infinite wavelength, and  $E_M$  is the "average" energy-gap parameter. The quantity  $E_M$ , which does not correspond to a real physical gap, is very similar to the energy parameter ("Penn gap") used by Penn<sup>14</sup> for the determination of the static refractive index in semiconductors: it is physically clear that  $E_M$  is a measure of the energy difference between the "centers of gravity" of the valence and conduction bands (Fig. 1). The determination of  $n_0$  and  $E_M$  from first principles, by the direct use of Eq. (2), is far too ambitious in the case of amorphous materials, where little is known on the transition probabilities of localized as well as extended band states. However, they can be derived from easily measurable properties of the material. As mentioned in Sec. III A, a two-parameter fit does indeed give an excellent fit to our experimental data. Furthermore,  $n_0$  can be obtained directly with a far-infrared spectrometer and we have verified for several samples that the result is the same as the extrapolated value from visible-light measurements.

The dispersion of the refractive index  $n(E)$  can be measured with a high precision from the maxima and minima of the Perot-Fabry oscillations, resulting in a precise measurement of the average gap  $E_M$ . The advantage of using the one-oscillator equation [Eq (3)] for the fit of

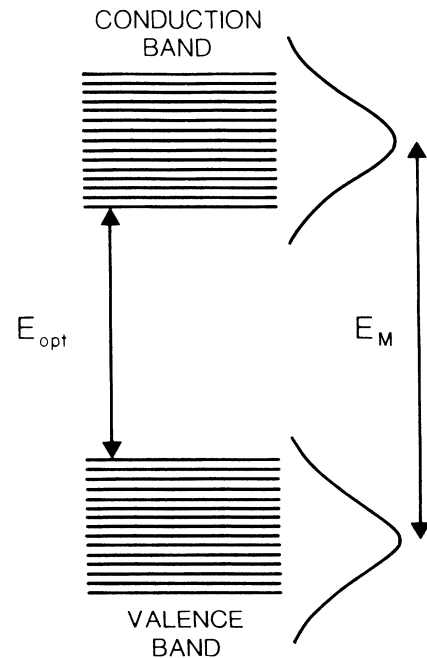


FIG. 1. Schematic diagram of the two-band model of a semiconductor. The dielectric response in the transparent region, i.e., for a light with energy  $E < E_{\text{opt}}$ , is very well approximated by a two-level system with an energy  $E_M$ . The "average gap"  $E_M$  is the distance between the centers of gravity of the valence and conduction bands with the appropriate weighting factors.

the experimental data is that it provides an intuitive physical interpretation of the measured quantities. In particular, the average gap  $E_M$  gives quantitative information on the overall band structure of the material. This is quite different from the information coming from the value of the optical gap  $E_{opt}$  which probes the optical properties near the band edges of the material. In particular, localized states near the conduction or valence band ("tail states") might have a strong effect on the optical absorption and thus decrease the optical gap, whereas if they have a small polarizability, they will result in a small effect on the refractive index: such tail states increase the "Urbach tail,"<sup>19,20</sup> but have little effect on the average gap  $E_M$ .

We show in Fig. 2 the variation of the refractive index  $n(E)$  for a series of samples with different carbon contents. As expected, the experimental variation of the refractive index departs from that given by Eq. (3) when the photon energy approaches the optical-gap value. Indeed, the one-oscillator approximation is valid only in the transparent region, in which the photon energy  $E$  is smaller than the optical gap. When  $E$  reaches the optical gap, there is some divergence due to the denominator terms in Eq. (2) and one would expect a variation of  $n(E)$  faster than that given by Eq. (3), which is indeed what is observed (Fig. 2).

We have measured the average gap  $E_M$  for a series of methylated amorphous silicon<sup>10,11</sup> samples. The results, as a function of the concentration of carbon (or methyl groups  $\text{CH}_3$ ) in the material, are given in Fig. 3. It is interesting to note how the average gap varies with the op-

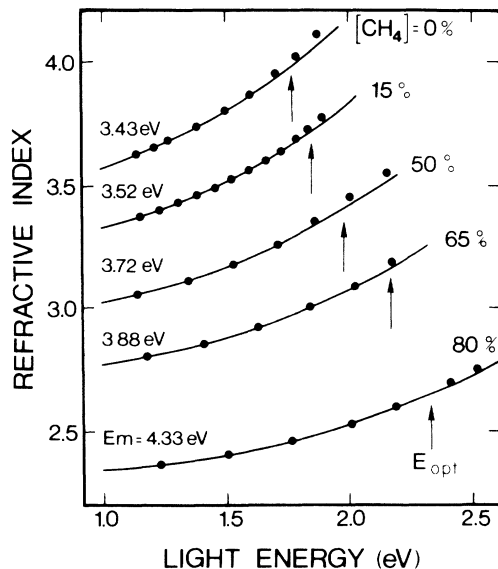


FIG. 2. Variation of the refractive index  $n$  with the light energy for a series of amorphous-silicon-carbon alloys with different carbon content. The materials were prepared from  $\text{SiH}_4\text{-CH}_4$  mixtures, the proportion of  $\text{CH}_4$  being indicated on the right. The variation of  $n$  is well verified by a one-oscillator formula [Eq. (3)] with an average gap  $E_M$ , except around the optical gap  $E_{opt}$  (vertical arrow) and beyond.

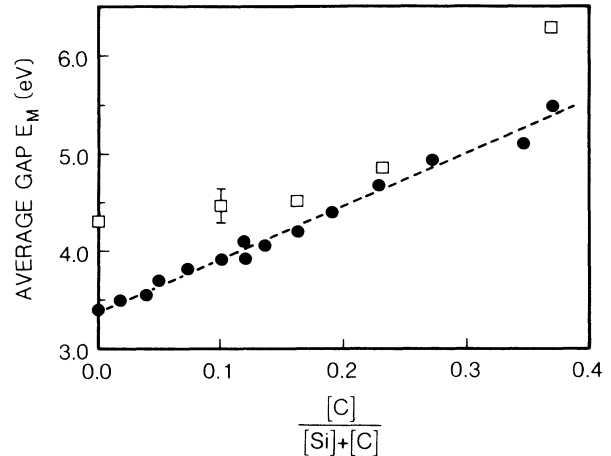


FIG. 3. The average gap  $E_M$  as a function of the carbon content in the solid for a series of silicon-carbon alloys. On the same diagram we have plotted (squares) the values of the distance between the peaks in the density of states of the valence and conduction bands as measured by soft-x-ray spectroscopy (SXS).

tical gap. Physically, it is clear that  $E_M$  should increase with the optical gap  $E_{opt}$  or with the equivalent measured parameter  $E_{04}$ . This is shown in Fig. 4, where we obtain, except for the highest concentrations of carbon, the empirical relation

$$E_M \cong 1.77E_{04} \quad (4)$$

indicating a scaling up of the overall band structure of

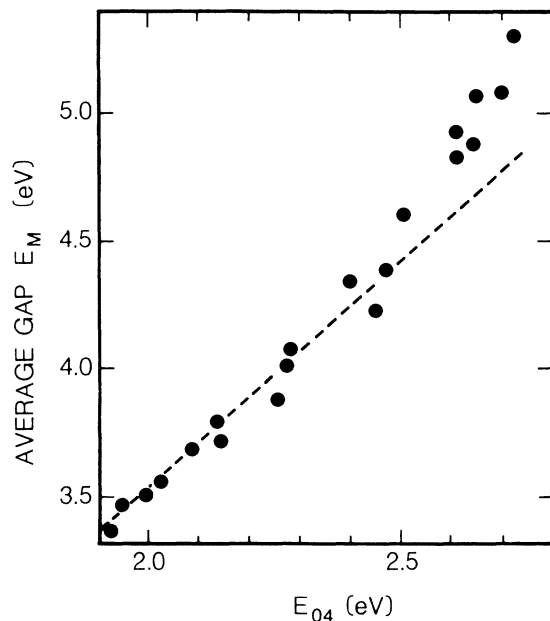


FIG. 4. The average gap  $E_M$  as a function of  $E_{04}$  (the photon energy corresponding to an absorption coefficient of  $10^4 \text{ cm}^{-1}$ ) for a series of silicon-carbon alloys with variable carbon content.

the material with carbon incorporation. Qualitatively, this is compatible with a scaling of all the transition energies with the increase of the average cohesive energy due to the progressive replacement of Si—Si bonds by the more stable Si—C bonds. This is in contrast with the simple tight-binding theory<sup>21–23</sup> which predicts, for elements of column IV, a variation given by

$$E_M \cong E_{04} + \Delta, \quad (5)$$

where  $\Delta$  is a constant energy of value between 1.5 and 2 eV. This equation is a direct result of the tight-binding approximation:<sup>21,23</sup> for  $sp^3$  bonds in crystals, the gap increases with the strength of the bond, whereas the widths of the valence and conduction bands remain constant. The source of the discrepancy between Eqs. (4) and (5) is not quite clear. The most likely explanation is that in our samples carbon is not incorporated as a carbon atom bounded to Si in a  $sp^3$  bond, but rather as a methyl group  $CH_3$ .

### C. Band structure studied by soft-x-ray spectroscopy (SXS)

The density of states (DOS) in the valence and conduction bands as a function of energy can be deduced from soft-x-ray spectra. A schematic energy diagram is displayed in Fig. 5. In x-ray-emission experiments, the sample is mounted on the anode of an x-ray tube, and the energy of x rays emitted from the sample corresponds to transitions from the valence band to the  $1s$  level. Transitions from the  $1s$  level to the conduction band are excited by absorption of x rays of corresponding energy. It is thus possible, from a combination of x-ray-emission and -absorption spectra, to reconstruct the band structure of the solid.

The result is shown in Fig. 6 for four samples with different carbon contents. The band structure of all samples is dominated by one major peak in each band. The energy difference  $E_p$  between the maxima of the valence-band and conduction-band peaks increases with carbon content. Qualitatively, the variation of  $E_p$  with the carbon concentration is similar to that of  $E_M$  (Fig. 3). This result confirms that the two-band model (Fig. 1) is a good approximation of optical transitions in amorphous silicon alloys. It justifies condensing the complicated theory of optical transitions into just one parameter, the average gap  $E_M$ . Our work shows, furthermore, that for our materials this important parameter can be obtained from optical transmission curves in a spectral range accessible with standard commercial spectrophotometers.

A precise quantitative agreement between  $E_p$  and  $E_M$  cannot be expected since the peak of the density of states in the valence or conduction band is not exactly the same as the weighted average in the two-band model, which takes into account both the density of states and the corresponding matrix elements of the transition probabilities. It should be noted that due to its rather low energy resolution (0.3–0.4 eV), SXS does not give reliable information on the optical gap, whereas this limited resolution does not affect the positions of the peaks in the band

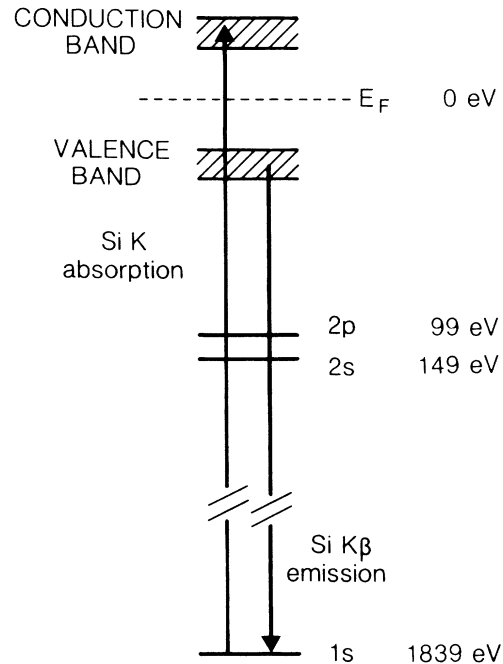


FIG. 5. Schematic diagram of the energy levels and transitions involved in SXS for silicon. Since the x-ray-emission and -absorption spectra concern the same core-level (Si  $1s$ ), the measured spectral distributions of the states in the valence and conduction bands directly give the energy positions of the band edges relative to the Fermi level. The position of the Fermi level is deduced from the Si  $1s$  binding energy obtained by combining the Si  $2p_{3/2}$  binding energy measured by XPS and the Si ( $2p_{3/2} \rightarrow 1s$ ) transition energy measured by SXS. The approximate energies between the silicon levels are indicated on the right.

structure. Beyond a carbon concentration of about 20 at.%, as shown in Figs. 4 and 6, anomalous properties are found: these could be related to the chemical structure and will be discussed in the following section.

### D. Chemical bonding studied by SXS and XPS

We have seen in the previous section that the energy gap between the maxima in the density of states of the valence and conduction bands accounts for the optical properties of our samples. The details of the shape of the density of states do not enter into the two-band model of optical transitions. However, the shape of the DOS contains information on the chemical structure of the solid. It is unfortunately very difficult to extract this information in terms of local bonding.<sup>24</sup>

The technique of x-ray-induced photoelectron spectroscopy probes the chemical environment of the atoms in the solid and is better adapted to the understanding of the band structure in terms of chemical interactions. We have analyzed by XPS the Si  $2p$  and C  $1s$  level distributions of three typical samples: a pure  $a$ -Si:H sample as a reference (sample A), a typical alloy with low carbon con-

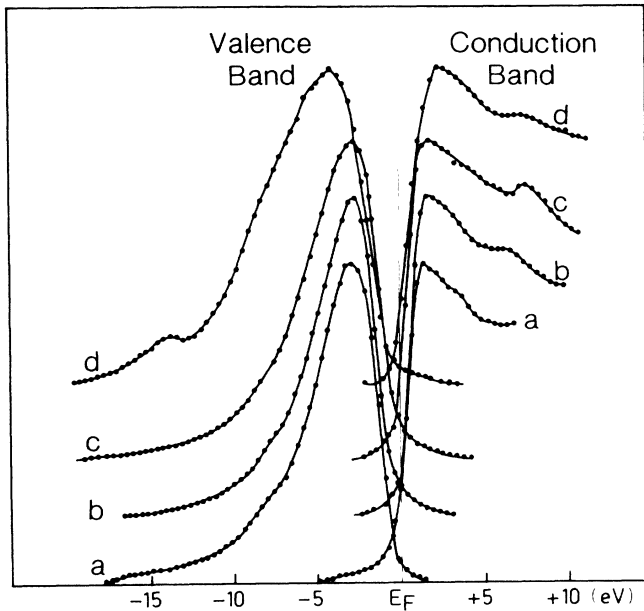


FIG. 6. Band structure obtained by a combination of x-ray-absorption and -emission spectra. The y axis (in arbitrary units) represents the intensity of Si  $K\beta$  emission (left) and the photoabsorption coefficient near the Si  $K$  absorption edge (right). Samples were prepared from  $\text{SiH}_4/\text{CH}_4$  mixtures containing (a) 60 at. %; (b) 75 at. %; (c) 85 at. %; (d) 95 at. % of methane, corresponding to carbon concentrations in the solid at 10 at. %, 16 at. %, 23 at. %, and 37 at. %.

tent  $a\text{-Si}_{0.84}\text{C}_{0.16}\text{:H}$  (sample B), and a high carbon content film  $a\text{-Si}_{0.66}\text{C}_{0.34}\text{:H}$  (sample C) which exhibits deviating optical properties. Our results, gathered in Table II, show that local order in films with low carbon content is very similar to that in pure  $a\text{-Si:H}$ . This explains why the DOS of the valence band for  $a\text{-Si}_x\text{C}_{1-x}$  films with low carbon concentrations is practically the same as in  $a\text{-Si:H}$ . Samples A and B have nearly the same Si  $2p$  binding energies; the presence of a few Si—C bonds in sample

B can be inferred from a component in the Si  $2p$  peak centered at 100.2 eV and from the C  $1s$  peak at 283.0 eV (Table II).

In sample C, silicon bonding is completely different: the line at 99.4 eV, indicating the presence of silicon atoms bonded to four other silicons (Si—Si<sub>4</sub> units), is absent, whereas it is predominant in samples A and B. Also, the energy shift of the C  $1s$  peak in sample C with respect to the corresponding peak in sample B points towards a modification of the chemical environment of carbon atoms, probably due to the simultaneous presence of Si—C and C—C bonds.

For this alloy, the DOS of the valence band is strongly modified (Fig. 6, curve *d*): the first peak is broadened by about 55% compared to  $a\text{-Si:H}$ , its maximum is shifted by 1.6 eV towards higher binding energies, and an additional peak is present at 13.7 eV from the Fermi energy  $E_F$ . This peak is also observed in crystalline SiC and its presence in sample C suggests the incorporation of tetrahedrally bonded carbon into the silicon network for the material with high carbon concentrations. The conduction band is less affected by carbon incorporation. The slope of the band edge decreases and the first maximum is shifted by 0.7 eV for a carbon concentration varying from  $x = 0$  to  $x = 0.34$ .

The results from XPS and SXS measurements suggest a qualitative correlation between the average gap and the chemistry of the carbon incorporation. The incorporation of small carbon concentrations only induces minor modifications of the silicon network. A few Si—C bonds are present, but there is no evidence for incorporation of the Si—C—Si type. This is consistent with the incorporation of carbon as methyl groups as postulated elsewhere.<sup>11</sup> The increase of the band gap is reflected in the density-of-state measurements as a receding of the valence-band edge.

Beyond a carbon content in the solid of about 20–25 at. %, stronger changes in chemical structure are observed. The chemical environment of silicon is completely changed and both Si—C and C—C bonds are detected. The strong changes in the  $p$  valence-band distribution can be due to the coexistence of carbon atoms with  $sp^3$  and

TABLE II. Binding energy  $E_B$  of Si  $2p$  and C  $1s$  states as obtained by numerical decomposition of XPS spectra.  $I_{rel}$  corresponds to the relative intensity of the peak components. For silicon, the XPS line at  $99.3 \pm 0.1$  eV (marked  $a\text{-Si}$ ) corresponds to the amorphous-silicon environment and the value at  $100.1 \pm 0.1$  eV (marked Si—C bond) indicates a bond between silicon and carbon in a tetrahedral network. The same bond gives rise to a carbon line at  $283.2 \pm 0.3$  eV, whereas an all-carbon tetrahedral environment (marked C—C bond) gives a carbon line at  $284.4 \pm 0.2$  eV (Ref. 25). The values in square brackets for samples B and C correspond to oxides and are due to the remaining surface contamination.

Sample	Si $2p$			C $1s$		
	$E_B$ (eV)	$I_{rel}$ (%)	Environment	$E_B$ (eV)	$I_{rel}$ (%)	Environment
A $a\text{-Si:H}$	99.3	100	$a\text{-Si}$			
B $a\text{-Si}_{0.84}\text{C}_{0.16}\text{:H}$	99.4	100	$a\text{-Si}$	283.0	100	Si—C bond
		6	Si—C bond	284.4	3	C—C bond
				[284.9]		
C $a\text{-Si}_{0.66}\text{C}_{0.34}\text{:H}$	100.1	100	Si—C bond	283.7	70	Si—C bond
	[101.4]	[28]		[285.0]	[100]	
	[102.4]	[15]				

$sp^2$  hybridization. The existence of strong disorder is indicated by the broadening of the valence and conduction-band edges. A displacement of the conduction-band edge towards higher energies contributes to the strong increase of the band gap.

#### IV. CONCLUSIONS

We have studied the optical properties and the band structure of a series of amorphous silicon-carbon alloys. In these films, produced by glow discharge in silane-methane mixtures at low power density, the carbon is mostly incorporated as methyl groups  $\text{CH}_3$ ,<sup>11</sup> and the optical properties of the films depend almost exclusively on the gas composition and are highly insensitive to the deposition parameters.<sup>10</sup> This material exhibits a wide range of optical properties, while disorder and defect density remains roughly constant. It thus provides an almost ideal model system for fundamental studies of band structure and optical properties of amorphous alloys.

We have not attempted to interpret from first principles the value of the *static* refractive index  $n_0$  that we have taken as a measured experimental parameter. In contrast, we have shown that the variation of the refractive index  $n(\lambda)$  with the wavelength  $\lambda$  (i.e., the dispersion of the sub-band-gap refractive index) is very well explained by a simple two-band model of optical transitions. The characteristic energy parameter in this model is the average gap  $E_M$ , the energy difference between the centers of gravity of the valence and conduction bands.

The variation of  $E_M$  with the carbon content gives a quantitative information on the overall band structure of the material. This information supplements the measured value of the optical gap  $E_{\text{opt}}$  which probes the optical properties near the band edges. Both the average gap  $E_M$  and the optical gap  $E_{\text{opt}}$  increase with increasing carbon content. This points towards a scaling of all transition energies with the increase of the average cohesive energy due to the progressive replacement of Si—Si bonds by the more stable Si—C bonds. However, the relative

variations of  $E_M$  and  $E_{\text{opt}}$  do not conform quantitatively to the simple tight-binding theory;<sup>23</sup> this might be due to the fact that in our samples carbon is incorporated in the random network as methyl groups  $\text{CH}_3$  rather than in the form of Si—C bonds.

More detailed information on the band structure in some of our samples has been obtained by SXS which directly gives the density of states of the valence and conduction bands. The peak-to-peak energy difference between the two bands is close to the average gap obtained from the optical dispersion curves, and it exhibits a similar increase with carbon content. We remark that both techniques, SXS and optical dispersion, give the same type of information on the band structure. Admittedly, SXS is more powerful since it gives the complete DOS curve, whereas the optical technique reduces the information to a single average parameter  $E_M$ . However, SXS not only has a rather poor resolution (0.3–0.4 eV), but is also a complex technique requiring high vacuum and special sample preparation. Our optical measurement of  $E_M$  is very simple and precise (resolution better than 50 meV), and combined with the optical gap  $E_{\text{opt}}$ , it provides a useful method for the study of amorphous alloys.

Beyond a carbon concentration of about 20 at.%, there is clear evidence of a change in the nature of the material and anomalous optical properties are observed. In particular, there is a very large enhancement of the average gap  $E_M$  which increases much faster than the optical gap  $E_{\text{opt}}$  (Fig. 4). X-ray photoelectron spectroscopy also reveals a change in the chemistry of the carbon incorporation: for low carbon concentrations, the carbon is mainly incorporated as methyl groups  $\text{CH}_3$ , whereas beyond a carbon concentration of about 20 at. % we observe a large incorporation of carbon in the form of Si-C-Si units in a tetrahedral network, even in the low-power regime.

#### ACKNOWLEDGMENT

This work has been partially supported by the European Community Contract No. EN3S=0062-F(CD).

\*Permanent address: SOLEMS S.A., 3 rue Léon-Blum, 91124 Palaiseau, France.

<sup>1</sup>C. Ance, J. P. Ferraton, J. M. Berger, and F. de Chelle, *Phys. Status Solidi B* **113**, 105 (1982), and references therein.

<sup>2</sup>J. Perrin, I. Solomon, B. Bourdon, J. Fontenille, and E. Ligeon, *Thin Solid Films* **62**, 327 (1979).

<sup>3</sup>G. D. Cody, C. R. Wronski, B. Abeles, R. B. Stephens, and B. Brooks, *Sol. Cells* **2**, 227 (1980).

<sup>4</sup>W. B. Jackson, S. M. Kelso, C. C. Tsai, J. W. Allen, and S.-J. Oh, *Phys. Rev. B* **31**, 5187 (1985).

<sup>5</sup>Y. Catherine, thesis, doctorat d'Etat, University of Nantes, 1981.

<sup>6</sup>R. S. Sussmann and R. Ogden, *Philos. Mag.* **B 44**, 137 (1981).

<sup>7</sup>Y. Catherine and A. Zamouche, *Plasma Chem. Plasma Process.* **5**, 353 (1985).

<sup>8</sup>K. D. MacKenzie, J. R. Eggert, D. J. Leopold, Y. M. Li, S.

Lin, and W. Paul, *Phys. Rev. B* **31**, 2198 (1985).

<sup>9</sup>J. Bullot and M. P. Schmidt, *Phys. Status Solidi B* **143**, 345 (1987).

<sup>10</sup>M. P. Schmidt, I. Solomon, H. Tran-Quoc, and J. Bullot, *J. Non-Cryst. Solids* **77-78**, 849 (1985).

<sup>11</sup>I. Solomon, M. P. Schmidt, and H. Tran-Quoc, *Phys. Rev. B* **38**, 9895 (1988).

<sup>12</sup>M. P. Schmidt, J. Bullot, M. Gauthier, P. Cordier, I. Solomon, and H. Tran-Quoc, *Philos. Mag.* **B 51**, 581 (1985).

<sup>13</sup>I. Solomon, M. P. Schmidt, C. Sénémaud, and M. Driss-Khodja, *J. Non-Cryst. Solids* **97-98**, 1091 (1987).

<sup>14</sup>D. R. Penn, *Phys. Rev.* **128**, 2093 (1962).

<sup>15</sup>C. Sénémaud and M. T. Costa Lima, *J. Non-Cryst. Solids* **33**, 141 (1979).

<sup>16</sup>J. Perrin, thesis, doctorat d'Etat, University of Paris, 1978.

<sup>17</sup>R. Swanepoel, *J. Phys. E* **16**, 1214 (1983).

- <sup>18</sup>S. H. Wemple and M. Didomenico, *Phys. Rev. B* **3**, 1338 (1971).
- <sup>19</sup>F. Boulitrop, J. Bullo, M. Gauthier, M. P. Schmidt, and Y. Catherine, *Solid State Commun.* **54**, 107 (1985).
- <sup>20</sup>A. Skumanich, A. Frova, and N. M. Amer, *Solid State Commun.* **54**, 597 (1985).
- <sup>21</sup>P. Manca, *J. Phys. Chem. Solids* **20**, 268 (1961).
- <sup>22</sup>H. Schade, Z. E. Smith, and A. Catalano, *Sol. Energy Mater.* **10**, 317 (1984), and references therein.
- <sup>23</sup>D. Weaire and M. F. Thorpe, *Phys. Rev. B* **4**, 2508 (1971).
- <sup>24</sup>T. M. Hayes, J. W. Allen, J. L. Beeby, and S. J. Oh, *Solid State Commun.* **56**, 953 (1985).
- <sup>25</sup>R. G. Cavel, S. P. Kowalczyk, L. Ley, R. A. Pollak, B. Mills, D. A. Shirley, and W. Perry, *Phys. Rev. B* **7**, 5313 (1973).